Proceedings of the XIth International Congress and Exposition
June 2-5, 2008 Orlando, Florida USA

Lateral force cantilever for precise atomic force microscope friction measurements

M.G. Reitsma*, R.S. Gates and R.F. Cook
Nanomechanical Properties Group
Materials Science and Engineering Laboratory
National Institute of Standards and Technology
100 Bureau Dr. Gaithersburg MD 20899 USA
*mark.reitsma@nist.gov

ABSTRACT

We present a microfabricated atomic force microscope (AFM) cantilever and associated calibration procedure that provide a path for quantitative friction measurement using a lateral force microscope. The lateral force cantilever is equipped with lever-arms that facilitate the application of normal and lateral forces, comparable to those acting in a typical AFM friction experiment. The cantilever allows for calibration and friction measurements to be carried out *in situ* and an AFM operator can select acceptable measurement precision via calibration measurements across the full working range of the instrument photodetector. We also identify and account for a misalignment susceptibility that could be encountered by operators using the calibration methods described. The lateral force cantilever is compatible with typical commercial AFM instrumentation and allows for common AFM techniques such as topography imaging and other surface force measurements to be performed.

INTRODUCTION

For more than two decades, the atomic force microscope (AFM) has been the principal instrument used for investigations of micro-to-nanoscale friction between solids [1]. So-called friction force microscope (FFM) measurements are usually performed either along the AFM cantilever long axis (*i.e.*, in the direction along the length of the cantilever) or perpendicular to it. While axial friction measurements—along the cantilever long axis—have been explored [2-5], the majority of FFM measurements are made perpendicular to the cantilever long axis (and probe) in a technique called lateral force microscopy (LFM).

AFM force measurement studies typically employ a probe that is either a small spherical solid attached to the cantilever free end (called a ‘colloidal probe’), or an integrated tip (fabricated as part of the cantilever). Fig. 1 shows a schematic diagram of an AFM cantilever with an integrated tip contacting an experimental surface of interest. Also depicted is a laser spot, reflected from the cantilever back side and incident on the four-sector optical Position Sensitive Detector (PSD) of the LFM instrument. The corresponding measurement data in Fig. 1 represents the PSD output as a function of the displacement of the surface (controlled piezoelectrically). Fig 1(a) shows an AFM force-displacement curve, used to calibrate the system for flexural deflection of the cantilever, where (i) is the out-of-contact *baseline* region; (ii) is the initial contact *snap-in* region; (iii) is the *compliance* region; and (iv) is the *pull-off* region, after which the surfaces separate again along (i). Fig. 1(b) shows typical LFM friction data, where scanning in one direction (i) and then the other (iii) produces hysteresis caused by frictional dissipation at the interface—called a ‘friction-loop’. Torsional deflection in the cantilever is caused by the frictional force at the interface acting through the lever-arm h. The half-width of this hysteric loop, ΔV_L (the ‘friction-loop half-width’), is proportional to the sliding resistance force due to friction. That is, a friction force, F_f, produces a torsional deflection in the cantilever that is proportional to the lateral PSD output, ΔV_L.

To quantify friction measurements in optical-lever LFM, the lateral output from the PSD, ΔV_L, needs to be related to the torsional moment, T, on the cantilever. While some promising techniques have employed force balance devices, which reportedly measure the lateral force response of a system directly [6, 7], the most commonly cited LFM calibration methods can be broadly classified as *wedge* and *lever methods*. Wedge methods either slide [8, 9] or press [10] the AFM cantilever probe against a known surface slope, where the mechanical response of the cantilever-probe on the incline is understood in terms of force balance equilibrium. Lever methods induce torsion by displacing a lever that has been attached (usually glued) to the AFM cantilever. The lever may be a stiff colloidal probe, for which torsion is induced via static friction between the probe and a stiff surface [11] or by pushing the equator of the sphere against another material [12, 13]. Another approach is to displace a beam that is attached orthogonally to both the cantilever long-axis and probe [14-17].

Many LFM calibration techniques proposed to date are so-called ‘two-step’ methods. That is, once the optical-lever system has been characterized for a torsional *deflection* of the cantilever (however determined), the torsional *stiffness* of the cantilever is required to complete the force calibration. The difficulty with two-step methods is that because the optical-lever response and the torsional spring constant are characterized in completely separate procedures, intrinsic uncertainties arise from the physical distinction between one procedure and the other. This difficulty is eliminated in the case of ‘single-step’ methods (such as wedge methods), where all variables in the calibration are present in a single calibration step, thus providing greater precision. The additional potential of a single-step method to yield accurate results is increased significantly for an *in situ* procedure in which a system calibration, along with a friction experiment, can be performed without dismantling or modifying the experimental setup.

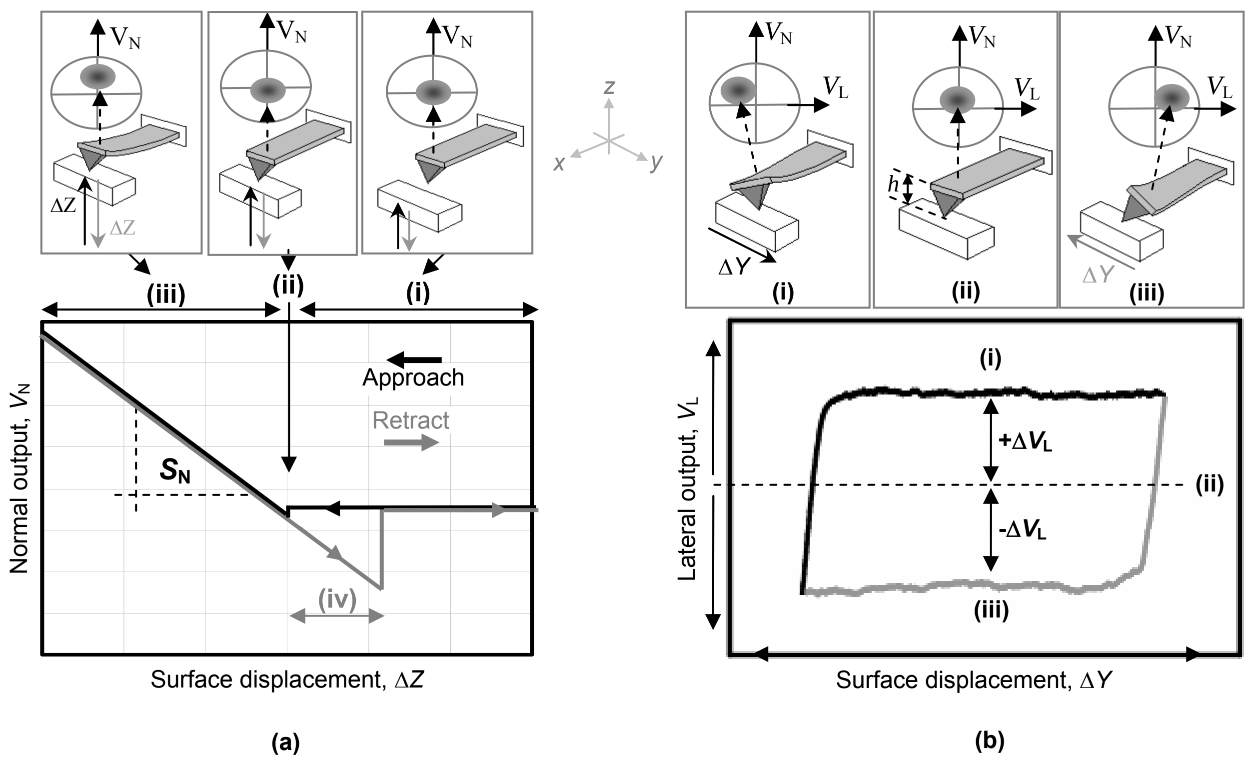

Figure 1. Typical AFM and LFM force data, showing (a) a ‘force-displacement curve’ and (b) a ‘friction-loop’

In this work, we describe the *in situ* method of Reitsma [18], which is based on the single-step—but not *in situ*—technique of Feiler *et al.* [15]. Firstly, we introduce a microfabricated prototype version of the “Hammerhead” cantilever proposed by Reitsma [18] and then demonstrate how it can be used to carry out calibration and friction measurements *in situ*. The calibration procedure generates an optical-lever sensitivity for lateral forces, which can be used to scale raw friction data for quantitative friction force measurements.

MATERIALS

Figure 2 shows one of the “Hammerhead” devices used for lateral force calibration in this work. Figure 2(a) shows a hammerhead cantilever without a probe. Figure 2(b) shows a hammerhead device “chip” (in wafer) carrying two cantilevers, one 500 µm and the other 300 µm in length, with both cantilevers 50 µm in width and 6 µm thick. Figure 2(c) shows a ramp-tab at the back end of the chip, with fiduciary marks used in calibration (see later). The devices were microfabricated using silicon-on-insulator wafers in which the device layer thickness controlled the thickness of the cantilever. The cantilevers were patterned through the device layer using photoresist and deep reactive ion etching (DRIE). The handle chip was defined by photoresist patterning and DRIE from the back side of the wafer. Final release of the cantilevers was achieved by dissolution of the buried oxide layer using hydrofluoric acid. A notched leg design (Figure 2(b)) was used to keep the handle chip securely attached to the wafer after release of the cantilevers. Finished chips were snapped out of the wafer for use.

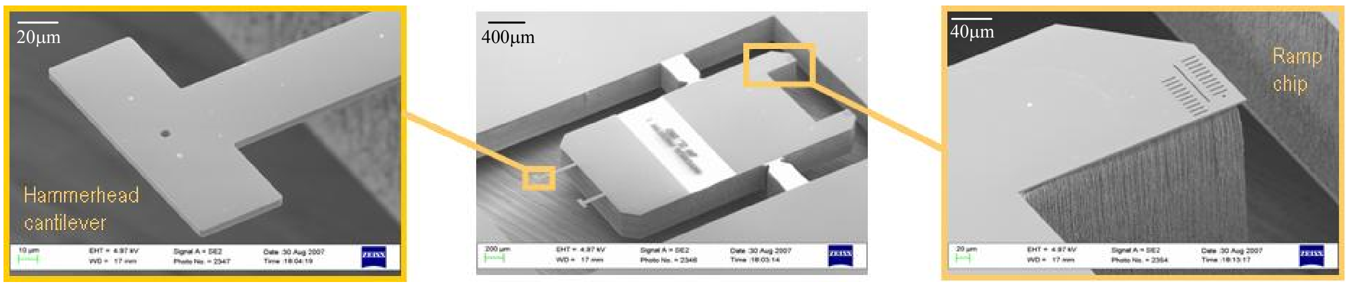

(a) **(b)** **(c)**

Figure 2. Scanning electron micrographs of the prototype “Hammerhead” chip showing: (a) a hammerhead cantilever; (b) a hammerhead chip still secured in the wafer; and (c) a ramp-tab at the back end of the chip.

CALIBRATION METHOD AND RESULTS

For the calibration technique described here, basic instrument requirements are an LFM-type (4-sector PSD) AFM that can be operated in force-displacement mode. The instrument must have top-down optics to view the experimental setup and also allow for coarse positioning of the cantilever or surface.

The hammerhead cantilever consists of three torsion lever-arms: the *experimental lever-arm* is simply the probe of the cantilever (which is used for friction experiments), and the two *calibration lever-arms,* orthogonal to both the probe and cantilever long-axis. Figure 3 shows perspective views of the experimental setup, which uses one chip as a “ramp chip” and another as a “cantilever chip”. In Figure 3(a), the experimental setup is such that the ramp chip is mounted onto the experimental surface of interest, allowing a friction experiment and instrument calibration to be carried out *in situ*, where coarse positioning of the cantilever or surface allows the operator to switch between experiment and calibration. Figure 3(b) depicts a calibration lever-arm positioned over a selected ramp-tab fiduciary mark during calibration. For the ramp-tab shown, fiduciary marks are 10 μm apart, and the lever-arm length H is formed through contact between the cantilever and chip edge. For the experimental setup used here, the piezo transducer moves the surface in the Z direction shown (‘up and down’). When the ramp chip contacts the lever-arm, the hammerhead cantilever will both twist (δ_M) and deflect flexurally (δ_Z). It should be noted that a relative angle between the cantilever and ramp chip can cause a mechanical crosstalk during calibration. Discussed in more detail later, this type of ‘system misalignment’ was eliminated by placing tungsten spheres on the ramp chip, such that contact was made between a calibration lever-arm and a (nominally) 50 µm diameter tungsten sphere (not pictured here).

Fig. 4 shows the three types of cantilever loading required for the hammerhead calibration. During loading, two types of LFM data are recorded: the top data sets are from the normal output, V_N, and the bottom sets are from the lateral output, V_L, of the PSD. The black trace in Fig. 4 represents a single (approach only) *force-displacement* curve (as in Fig. 1(a)), where for an assumed rigid probe-surface contact and elastic cantilever deflection, the *normal sensitivity*, S_N (= $\Delta V_N/\Delta Z$) is the change in normal PSD output, ΔV_N, as a function of surface displacement,

ΔZ. In this case, an applied force, F_Z, can be determined from the flexural spring constant of the cantilever, k_Z, such that [19]

$$F_Z = \frac{k_Z \Delta V_N}{S_N} \quad (1)$$

The grey traces in Fig. 4 represent *torque-displacement* curves (approach only), generated by pressing one calibration lever-arm and then the other at lever-arm lengths $H_+ = H_- = [65 \pm 0.5]$ μm, measured using the overhead optics of the AFM [20]. Pressing the right lever-arm ($H_+ \rightarrow +V_L$) gives the light-grey trace and the left ($H_- \rightarrow -V_L$) gives the dark-grey trace. As expected for a well-aligned system, the force-displacement curve (black trace) remains zero in the lateral output plot and both torque-displacement curves (grey traces) overlap on the normal output plot for the entire ramp range of the piezo.

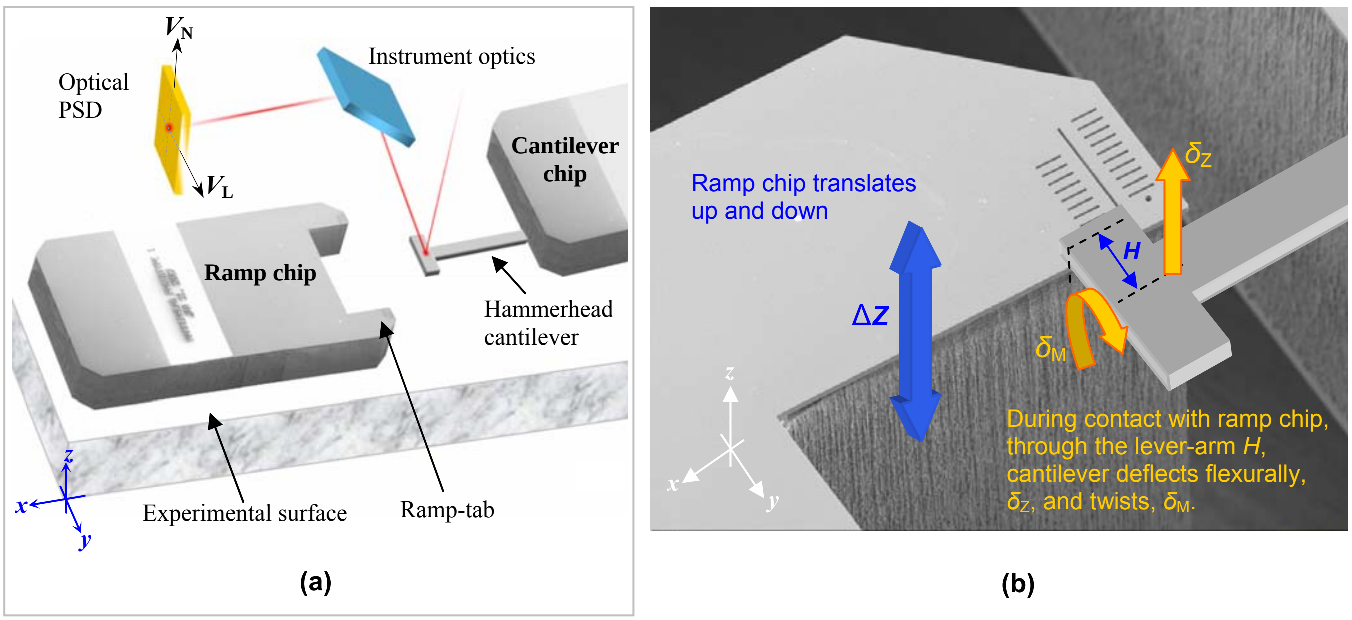

Figure 3. Depiction of experimental setup, showing (a) a ramp chip mounted onto an experimental surface, allowing for *in situ* calibration and friction measurement; and (b) a ramp-tab and hammerhead cantilever.

Good linearity of all data in Fig. 4 means that the ratio between normal and lateral PSD output signals—the *PSD output ratio* (V_L/V_N)—remained constant over the entire range of displacement. Two essential requirements for the calibration technique are (1) all calibration data are collected within the linear range of the PSD; and (2) there is negligible coupling between flexural and torsional spring constants in the cantilever for the very small degrees of cantilever twist (<< 1°) relevant here. Under these conditions, since a force, F_Z, applied at a calibration lever-arm distance, H, will cause the hammerhead cantilever to deflect flexurally as well as twist, we can quantify F_Z by observing the flexural deflection response of the cantilever. In this case, we use Equation 1 to describe a lateral force, F_Z, applied to a calibration lever-arm in terms of a torque, $T = F_Z H$, such that

$$T = \frac{k_Z \Delta V_N H}{S_N} \quad (2)$$

The central problem in quantifying friction measurements in LFM is to relate ΔV_L to T. We could thus define a torsional parameter, which we will call the *Lateral Force Sensitivity (LFS)*, S_γ, as

$$S_\gamma = \frac{\Delta V_\mathrm{L}}{T} \qquad (3)$$

Combining Equations (2) and (3), we can write

$$\left(\frac{\Delta V_\mathrm{L}}{\Delta V_\mathrm{N}}\right) = S_\gamma \left(\frac{H k_\mathrm{Z}}{S_\mathrm{N}}\right) \qquad (4)$$

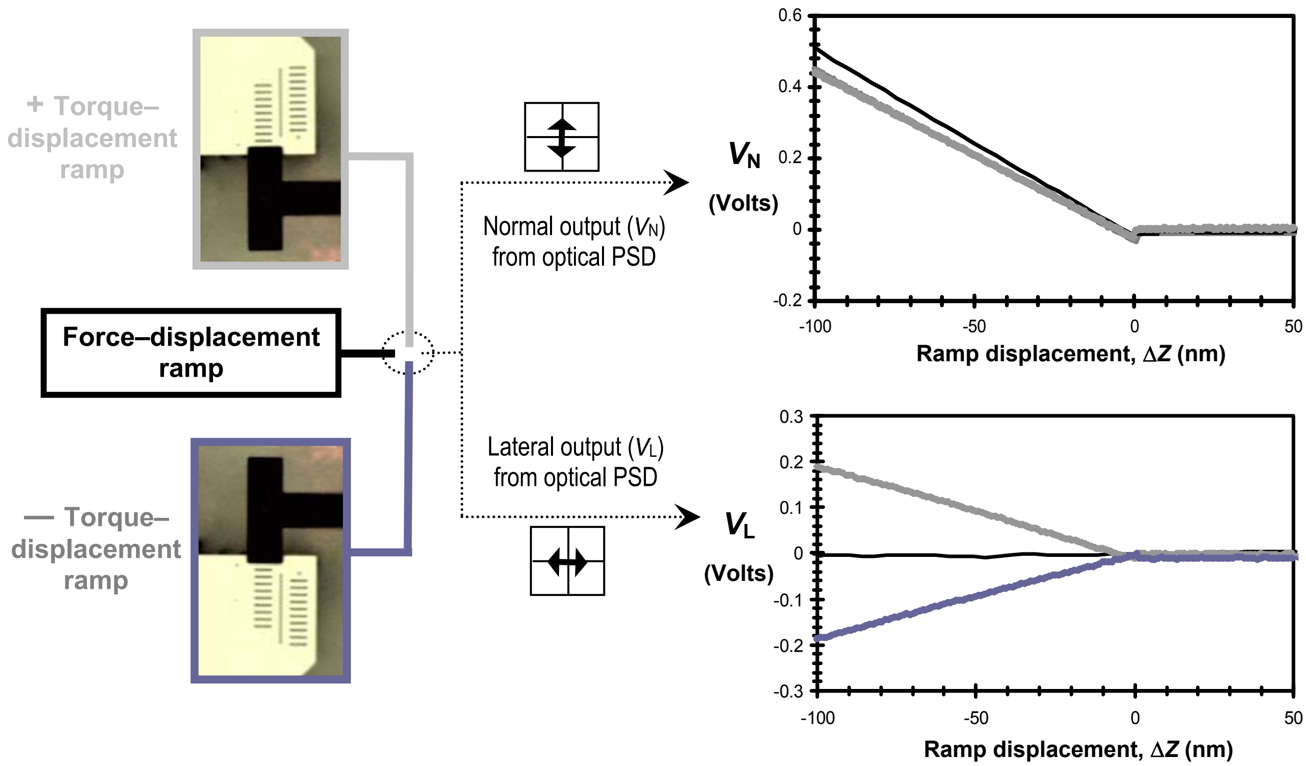

Figure 4. Hammerhead calibration data for H = 65 μm

From Equation 4, it can be seen that for a series of different lever arm lengths, H, a plot of $V_\mathrm{L}/V_\mathrm{N}$ versus $Hk_\mathrm{Z}/S_\mathrm{N}$ should give a straight line of slope S_γ. Fig. 5 below was obtained in this way by collecting calibration measurements (as in Fig. 4) for different values of H. From Fig. 5, an LFS of S_γ = [9.15 ± 0.08] x10^9 V $(\mathrm{Nm})^{-1}$ was obtained from a linear regression slope fit to the data [20]. Note that the PSD output ratio ($V_\mathrm{L}/V_\mathrm{N}$) of force-displacement data are plotted at H = 0. A linear LFS plot that passes through the origin and includes both H = 0 and $H \neq 0$ data—as in Fig. 5—is a good indication of a system that is well aligned. The susceptibility of the current method to system misalignment ('crosstalk') is the subject of ongoing investigation. Positioning uncertainty in H, measured through the overhead optics of the AFM, is presumably the major source of scatter in the Fig. 5 data. The normal sensitivity of the system, S_N, used for the LFS calibration (see abscissa term in Fig. 5), is the average S_N value for eight force-displacement curves, collected regularly throughout the experiment. Also note that the data points in color in Fig. 5 correspond to the data shown in Fig. 4.

Force enters the LFS calibration through the flexural stiffness of the cantilever, and so the accuracy of the force calibration is predicated on the accuracy of this property measurement. For the data presented here, the flexural stiffness of the hammerhead cantilever was estimated to be 4.1 Nm^{-1} from finite element modeling using nominal cantilever dimensions. In future, flexural stiffness will be measured initially using an instrumented indenter technique [21], and later determined using SI-traceable methods [22, 23].

Figure 5.

Lateral Force Sensitivity (LFS) calibration.

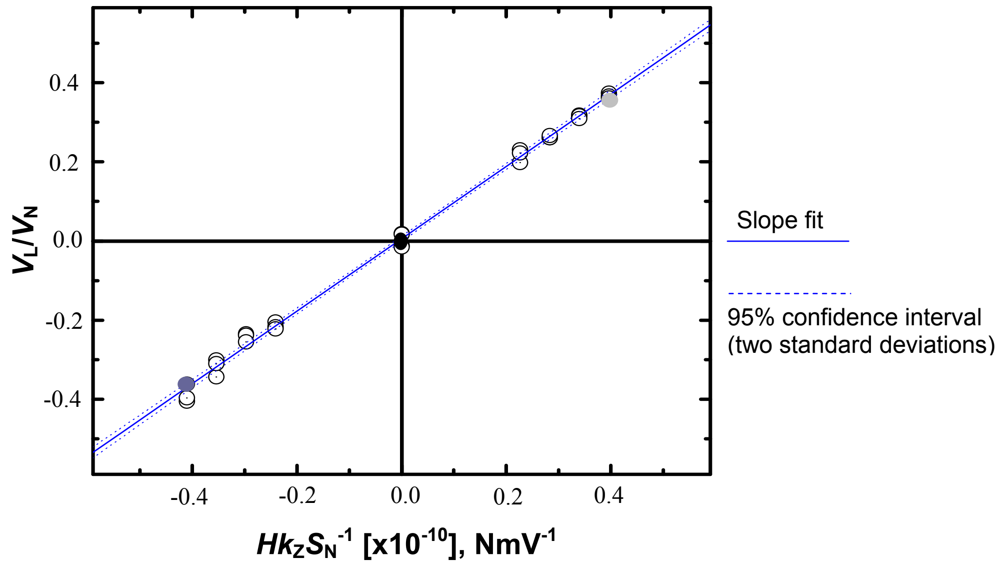

The LFS, S_γ, is essentially an optical-lever sensitivity for lateral forces, which can be used to scale raw friction data. Referring to the friction-loop in Figure 1(b), if the length of the cantilever probe, h, is the (z) distance from the neutral axis of the cantilever (about which twisting occurs) to the probe-surface contact where the friction force, F_f, is acting, then the torsional moment on the cantilever will be $T = F_f h$. The lateral output during a friction experiment, ΔV_L (i.e. 'friction-loop half-width') can then be used to quantify the friction force using Equation (3), once the LFS of the system has been calibrated.

SYSTEM MISALIGNMENT

'Crosstalk' is a typical and almost unavoidable issue in LFM, arising from misalignment in the experimental setup. *Optical crosstalk* is caused by a misalignment between the (reflective) surface normal of the cantilever and the sector axis of the PSD. The LFS parameter for this method (*i.e.*, the slope of the fit in Fig. 5) has a negligible susceptibility to optical crosstalk because the optical response of the system to torque in the cantilever is accounted for across the working range of the photodiode. *Mechanical crosstalk* can be induced by a misalignment between the surface normal of the sample (the ramp chip in this case) and the surface normal of the cantilever. The calibration technique presented here can give important information about crosstalk misalignment for a particular experimental setup. Referring to the LFS plot in Fig. 5, a linear fit that includes both $H \neq 0$ and $H = 0$ data is a good indication of minimal mechanical crosstalk in the system, and furthermore, any ordinate off-set in such a linear LFS plot would likely be due to optical crosstalk, the magnitude of which is given by the ordinate at $H = 0$. In any case, a linear LFS plot that passes through the origin is a good indication of a system in which all crosstalk has been minimized. Fig. 5 had an average offset of $[V_L/V_N]_{H=0} = 0.002 \pm 0.018$.

As mentioned earlier, mechanical crosstalk was minimized here by loading the torsion lever-arms against tungsten spheres (for $H \neq 0$ data) that were glued on the edge of the ramp-tab (not shown). Before attaching tungsten spheres, however, a calibration was performed on the bare ramp-tabs. The effect of misalignment between cantilever and ramp chip on LFS calibration data can be seen in Fig. 6. The perspective of each illustration—(a), (b) and (c)—is looking down the long axis (from the fixed to the free end) of the cantilever, which is shaded grey. Note that the relative angle between the cantilever and chip (typically < 1°) has been exaggerated for clarity. We are also looking directly at the ramp-tabs at the back of the ramp chip (the fiducial marks on each tab are also shown). In (b) and (c), the eye represents the view of the top-down optics, which does not allow detection of this type of misalignment. The effect of the misalignment can be seen in the experimental calibration data shown in Fig. 6. While misalignment does not appear to affect the negative H (grey data) ramp, in (b), there is no change in the PSD output ratio response as a function of lever-arm length for the postive H (black data) ramp, in (c). This is because, through the overhead optics, four different lever-arm lengths were apparently used, but the actual length each time was the total length of the lever-arm (H_{max} = 75 μm), as illustrated in Fig. 6(c). The star is the expected (non-experimental) datum point for the lever-arm, H_{max}, generated by taking the average V_L/V_N of each of the experimental values (black circles). The open circles at H = 0 are force-displacement ramps.

The linear fit that includes the negative lever-arm (grey) data, the zero lever-arm (open circle) data, as well as the non-experimental (star) point at H = 75 μm demonstrates how compensation can be made for this type of system misalignment. From the linear fit shown in Fig. 6, the lever-arm sensitivity of [5002 ± 330] m^{-1}, is comparable to that for the system in which tungsten spheres were used in Fig. 5 [5190 ± 143] m^{-1} [20]. This compensation for misalignment demonstrates that the calibration method presented here can be performed without the need to attach or use any additional materials, other than the hammerhead cantilever and ramp chip.

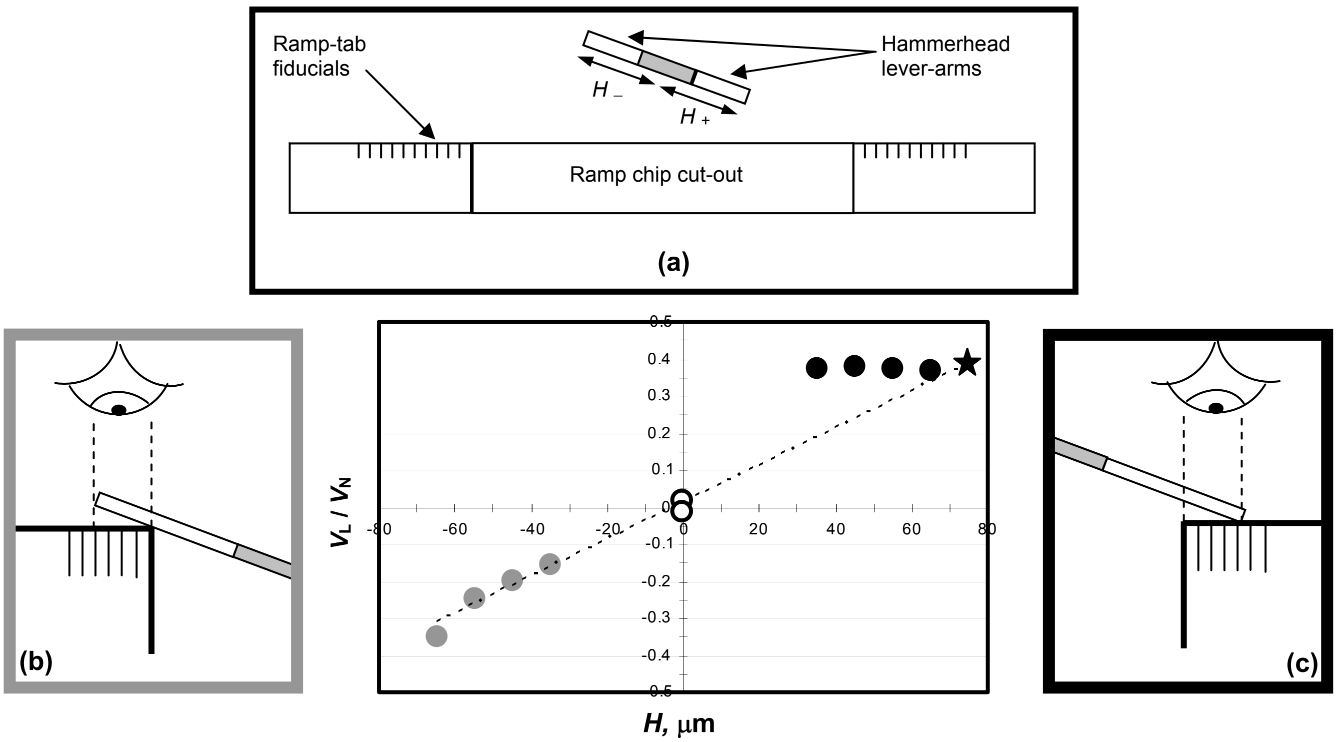

Figure 6. Effect of misalignment between cantilever and ramp chip on LFS calibration data (angles are exaggerated for clarity).

CONCLUSION

We have presented a microfabricated device and calibration procedure that provide a path for quantitative friction measurement using a lateral force microscope. The lateral force cantilever allows for calibration and friction measurements to be carried out *in situ* and an operator can select acceptable precision via measurements across the full working range of the instrument photo-detector. The calibration method generates an optical-lever sensitivity for lateral forces, which can be used to scale raw friction data. We have identified and compensated for a misalignment susceptibility that could be encountered by operators using this method. The microfabricated hammerhead chip presented here is compatible with typical commercial AFM instrumentation. In the near future, we will be fabricating hammerhead cantilevers with integrated tips, which will allow for common AFM techniques such as topography imaging and other surface force measurements to be performed. True force measurement accuracy for this cantilever—via Système International (SI) traceability [22, 23]—has also been planned in future work.

REFERENCES

1. Mate CM, McClelland GM, Erlandsson R, Chiang S (1987) Atomic-scale friction of a tungsten tip on a graphite surface. Phys. Rev. Lett. 59(17):1942-1945.
2. Ruan JA, Bhushan B (1994) Atomic-Scale Friction Measurements using Friction Force Microscopy: Part I - General Principles and New Measurement Techniques. ASME J. Tribology 116:378-388.
3. Watson GS, Dinte BP, Blach-Watson JA, Myhra S (2004) Friction measurements using force versus distance friction loops in force microscopy. App. Surf. Sci. 235:38-42.
4. Stiernstedt J, Rutland MW, Attard P (2005) A novel technique for the in situ calibration and measurement of friction with the atomic force microscope. Rev. Sci. Instrum. 76:083710.
5. Stiernstedt J, Rutland MW, Attard P (2006) Erratum: Rev. Sci. Instrum. 76, 083710 (2005). Rev. Sci. Instrum. 77:019901.
6. Cumpson PJ, Hedley J, Clifford CA (2005) Microelectromechanical device for lateral force calibration in the atomic force microscope: Lateral electrical nanobalance. J. Vac. Sci. Technol. B 23(5):1992-1997.
7. Li Q, Kim K-S, Rydberg A (2006) Lateral force calibration of an atomic force microscope with a diamagnetic levitation spring system. Rev. Sci. Instrum. 77:065105.
8. Ogletree DF, Carpick RW, Salmeron M (1996) Calibration of frictional forces in atomic force microscopy. Rev. Sci. Instrum. 67(9):3298-3306.
9. Varenberg M, Etison I, Halperin G (2003) An improved wedge calibration method for lateral force in atomic force microscopy. Rev. Sci. Instrum. 74(7):3362-3367.
10. Assay DB, Kim SH (2006) Direct force balance method for atomic force microscopy lateral force calibration. Rev. Sci. Instrum. 77:043903.
11. Cain RG, Biggs S, Page NW (2000) Force calibration in Lateral Force Microscopy. J. Colloid Interface Sci. 227:55-65.
12. Ecke S, Raiteri R, Bonaccurso E, Reiner C, Deiseroth H-J, Butt H-J (2001) Measuring normal and frictional forces acting on individual fine particles. Rev. Sci. Instrum. 72(11):4164-4170.
13. Cannara RJ, Eglin M, Carpick RW (2006) Lateral force calibration in atomic force microscopy: A new lateral force calibration method and general guidlines for optimization. Rev. Sci. Instrum. 77:053701.
14. Toikka G, Hayes RA, Ralston J (1997) The application of lateral force microscopy to particle removal in aqueous polymer solutions. J. Adhesion Sci. Technol. 11(12):1479-1489.
15. Feiler A, Attard P, Larson I (2000) Calibration of the torsional spring constant and the lateral photodiode response of frictional force microscopes. Rev. Sci. Instrum. 71(7):2746-2750.
16. Bogdanovic G, Meurk A, Rutland MW (2000) Tip friction - torsional spring constant calibration. Colloids and Surfaces B: Biointerfaces 19:397-405.
17. Instead of attaching a beam to the cantilever, Bogdanovic et al (Ref. [16]) apply torsion by pressing a protuberance against the edge of the cantilever so that the applied force is off-set laterally from the center of the cantilever long axis.
18. Reitsma MG (2007) Lateral force microscope calibration using a modified atomic force microscope cantilever. Rev. Sci. Instrum. 78:106102.
19. Since an AFM cantilever is typically mounted at an angle (*e.g.* approximately 10º) relative to a nominal planar surface, a geometrical correction is required to resolve force in the Z direction. This correction (typically 3% to 4%) is ignored for all Z forces in this paper.
20. Unless otherwise stated, all uncertainties represent 95% confidence limits (two standard deviations); except dimensional measurements using optical microscopy, where uncertainty is the optical resolution of the device used in this work.
21. Ying ZC, Reitsma MG, Gates RS (2007) Direct Measurement of Cantilever Spring Constants and Correction of Cantilever Irregularities using an Instrumented Indenter. Rev. Sci. Instrum. 78:063708.
22. Gates RS, Pratt JR (2006) Prototype cantilevers for SI-traceable nanonewton force calibration. Meas. Sci. Technol. 17:2852-2860.
23. Gates RS, Reitsma MG (2007) Precise AFM Cantilever Spring Constant Calibration using a Reference Cantilever Array. Rev. Sci. Instrum. 78:086101.